Development 139, 191-202 (2012) doi:10.1242/dev.070151

miR-200c regulates FGFR-dependent epithelial proliferation via Vldlr during submandibular gland branching morphogenesis

Ivan T. Rebustini[1], Toru Hayashi[1], Andrew D. Reynolds[1], Melvin L. Dillard[1], Ellen M. Carpenter[2] and Matthew P. Hoffman[1,*]

SUMMARY

The regulation of epithelial proliferation during organ morphogenesis is crucial for normal development, as dysregulation is associated with tumor formation. Non-coding microRNAs (miRNAs), such as miR-200c, are post-transcriptional regulators of genes involved in cancer. However, the role of miR-200c during normal development is unknown. We screened miRNAs expressed in the mouse developing submandibular gland (SMG) and found that miR-200c accumulates in the epithelial end buds. Using both loss- and gain-of-function, we demonstrated that miR-200c reduces epithelial proliferation during SMG morphogenesis. To identify the mechanism, we predicted miR-200c target genes and confirmed their expression during SMG development. We discovered that miR-200c targets the very low density lipoprotein receptor (Vldlr) and its ligand reelin, which unexpectedly regulate FGFR-dependent epithelial proliferation. Thus, we demonstrate that miR-200c influences FGFR-mediated epithelial proliferation during branching morphogenesis via a Vldlr-dependent mechanism. miR-200c and Vldlr may be novel targets for controlling epithelial morphogenesis during glandular repair or regeneration.

KEY WORDS: miR-200c, Vldlr, Salivary gland, Mouse

INTRODUCTION

MicroRNAs (miRNAs) are small non-coding RNAs that target multiple messenger RNAs (mRNAs) and function as post-transcriptional regulators of gene expression. They have emerged as key regulators of proliferation (Wang, S. et al., 2008), apoptosis (Fujita et al., 2009), maintenance of progenitor cell identity (Marson et al., 2008) and embryonic stem cell fate (Tiscornia and Izpisua Belmonte, 2010). During development, miRNAs regulate skin (Yi et al., 2006), blood vessel (Wang, S. et al., 2008) and neuronal (Yoo et al., 2009) morphogenesis, and the expression of multiple miRNAs in the developing lung (Wang et al., 2007) and submandibular gland (SMG) (Jevnaker and Osmundsen, 2008; Hayashi et al., 2011) suggests that they regulate gene expression associated with development; however, the functional characterization of miRNAs during epithelial branching morphogenesis remains to be elucidated.

miR-200c is among the miRNAs implicated in disease, and a reduction in miR-200c expression is associated with multiple cancers that have invasive cell phenotypes (Burk et al., 2008). A direct target of miR-200c is *Zeb1*, a transcriptional repressor of E-cadherin in epithelial cells (Gregory et al., 2008). A decrease in miR-200c expression increases *Zeb1*, which downregulates E-cadherin, thus increasing epithelial-to-mesenchyme transition (EMT) during tumor transformation (Gregory et al., 2008). Conversely, decreasing *Zeb1* expression upregulates E-cadherin and inhibits EMT (Park et al., 2008). Zeb1 also promotes tumor formation by reducing the expression of miR-200c, which cooperates to suppress stem cell factors in cancer. Additionally, miR-200c strongly suppresses cell proliferation of human breast cancer stem cells during tumor initiation in vivo (Shimono et al., 2009). Therefore, an inverse correlation between miR-200c expression and cell proliferation occurs during cancer formation, but it is not known whether this also occurs during normal organ morphogenesis.

A connection between miR-200c and low density lipoprotein receptors (LDLRs) has not been previously described. LDLRs bind to apolipoproteins that regulate vasculogenesis (Oganesian et al., 2008) and lipid metabolism in adipocytes (Yin et al., 2008) and hepatocytes (Sanderson et al., 2010). Among the LDLRs, very low density lipoprotein receptor (Vldlr) and apolipoprotein-E receptor 2 (ApoER2; also known as Lrp8) bind to the extracellular matrix protein reelin (Reln), and induce neuronal migration and layering of the cerebral cortex (Trommsdorff et al., 1999; Cariboni et al., 2005) via PI3K (Jossin and Goffinet, 2007) and ERK1/2 phosphorylation (Webb et al., 1999). Knockout mice for *Vldlr*, *Reln* or *Dab1*, which encodes the intracellular adaptor protein that mediates reelin/Vldlr signaling, are viable with similar neurological phenotypes, and the deletion of *Reln* or *Dab1* was recently reported to decrease terminal branching, duct elongation and luminal organization during mammary morphogenesis (Khialeeva et al., 2011). However, the mechanisms that regulate Vldlr function during epithelial morphogenesis remain to be elucidated.

Epithelial organs such as SMGs develop by branching morphogenesis, which requires coordinated proliferation and differentiation of the epithelium in order to form a complex branched structure (Patel et al., 2006; Walker et al., 2008). During this process, proliferation is localized predominantly in the epithelial end buds and is induced by multiple signaling pathways, including muscarinic receptors (Knox et al., 2010), FGFRs

[1]Matrix and Morphogenesis Section, Laboratory of Cell and Developmental Biology, National Institute of Dental and Craniofacial Research, National Institutes of Health, Bethesda, MD 20892, USA. [2]Department of Psychiatry and Biobehavioral Science, UCLA School of Medicine, Los Angeles, CA 90095, USA.

*Author for correspondence (mhoffman@mail.nih.gov)

Accepted 18 October 2011

(Hoffman et al., 2002), EGFRs (Steinberg et al., 2005; Rebustini et al., 2009) and PDGFRs (Yamamoto et al., 2008). By contrast, less is known about the mechanisms that restrict or decrease epithelial proliferation at discrete locations and stages of development so that normal branching morphogenesis can occur.

We have discovered that miR-200c decreases FGFR-dependent epithelial proliferation via regulation of Vldlr function during SMG branching morphogenesis. Our observations provide mechanistic insight into how miR-200c counterbalances proliferation during normal epithelial morphogenesis, and unveil an unexpected role for its target genes, *Vldlr* and *Reln*, in regulating FGFR-dependent epithelial proliferation during branching morphogenesis.

MATERIALS AND METHODS

SMG organ and epithelial cultures

SMGs were harvested from embryonic day (E) 12 or E13 ICR mice (Harlan, Frederick, MD, USA) and the epithelia were separated from the mesenchyme and cultured as previously described (Rebustini and Hoffman, 2009). The epithelia were cultured with 400 ng/ml Fgf10 and 100-500 ng/ml reelin (both from R&D Systems, Minneapolis, MN, USA), function-blocking Vldlr antibody (R&D Systems, 0.5 μM) (D'Arcangelo et al., 1999; Sinagra et al., 2005) and 0.5 μg/ml heparan sulfate (Sigma, St Louis, MO, USA). *Dab1*^{exKIneo} mice have been described previously (Khialeeva et al., 2011).

Screening of miRNA expression using TaqMan low density arrays

Total RNA and the Megaplex Pools protocol and reagents (Applied Biosystems, Foster City, CA, USA) were used to detect miRNA expression. Briefly, cDNA was synthesized using total RNA and Megaplex RT, followed by a pre-amplification step and PCR detection using TaqMan low density array (TLDA, miRNA mouse pool A, Applied Biosystems) containing primers for 377 mouse miRNAs and the housekeeping gene snRNA-U6. The data were analyzed using SDS Database System 2.3 (Applied Biosystems), and RealTime StatMiner software (Integromics, Philadelphia, PA, USA). Relative fold change in miRNA expression was calculated comparing the cycle threshold (CT) numbers of each detected miRNA with snRNA-U6, and comparing differences in CTs between the E13 SMG epithelium and mesenchyme, and the E13 SMG epithelial end buds and main duct. A fold change of 2.0 was defined as a threshold for significant change in expression, and miRNAs detected with CT values above 32 were defined as undetectable.

Transfection of antagomirs and miRNA mimics during SMG and epithelial cultures

The miRCURY LNA-based control, the miR-34a, miR-200c, miR-204 and miR-135a antagomir inhibitors (Exiqon, Vedbaek, Denmark), and the miScript miR-200c mimic (Qiagen, Valencia, CA, USA) were transfected at 400 nM in E12 SMG organ cultures and in E13 SMG epithelia using RNAiFect (Qiagen), as previously described (Rebustini et al., 2009). DNase-free total RNA was prepared using micro-RNAqueous and mirVana miRNA isolation kits (Ambion, Austin, TX, USA).

Quantitative (q) PCR analysis

Total RNA samples were DNase treated (Ambion) prior to cDNA synthesis using iScript reagents (BioRad, Hercules, CA, USA). SYBR-Green qPCR was performed using 1 ng cDNA and primers designed using Beacon Designer software (supplementary material Table S1). Melt-curve and primer efficiency analyses were performed as previously described (Hoffman et al., 2002). Gene expression was normalized to *Rps29* and to the corresponding experimental control, and reactions were run in triplicate and independently repeated three times. For miRNA-200c expression analysis, the Universal RT miRNA-cDNA synthesis kit, LNA-modified oligonucleotides and the miRCURY microRNA PCR System (Exiqon) were used. Gene expression was normalized to the housekeeping gene snRNA-U6 and to the corresponding experimental group control. For analysis of the miR-200 family the mirVana miRNA isolation kit was used and TaqMan microRNA assays (Applied Biosystems) were used for miR-200a, miR-200b, miR-200c, miR-141 and miR-429. Expression was normalized to the housekeeping gene snRNA-U6 and the experimental control, and another housekeeping gene, snoRNA202, was included.

Detection of proliferation and immunofluorescence analysis

Cell proliferation was detected using Click-iT EdU Imaging Systems (Invitrogen, Carlsbad, CA, USA). Briefly, SMGs were incubated with EdU for 30 minutes, fixed in 1:1 acetone:methanol or 4% paraformaldehyde (PFA), and incubated with a Click-iT EdU reaction cocktail for 30 minutes. After EdU detection, the tissue was washed and blocked for 1 hour in 10% heat-inactivated donkey serum, 1% BSA, MOM IgG blocking reagent (Vector Laboratories, Burlingame, CA, USA), prior to overnight incubation at 4°C with a rabbit primary anti-rat E-cadherin antibody (Sigma). The SMGs were washed in PBS-T (PBS containing 0.2% Tween 20) and the antibodies were detected using Cy3- or Cy5-conjugated secondary Fab fragment antibodies (Jackson Laboratories, Bar Harbor, ME, USA). Fluorescence was analyzed using a Zeiss 510 laser-scanning microscope (Zeiss, Thornwood, NY, USA) and quantified and normalized to epithelial area as previously described (Rebustini et al., 2007).

In situ hybridization

SMGs were cultured for 2 hours, fixed in 4% PFA in PBS for 20 minutes, and used for in situ hybridization (ISH) as previously described (Kloosterman et al., 2006). Briefly, the embryonic organs were bleached in 0.6% H_2O_2 for 30 minutes, permeabilized with 10 μg/ml proteinase K for 15 minutes, post-fixed with 4% PFA and 0.3% glutaraldehyde for 15 minutes, pre-incubated with hybridization buffer for 3 hours, incubated with 7.5 pmol DIG-labeled LNA-modified miR-200c probe (Exiqon) and diluted in 0.7 ml hybridization buffer. Positive and negative probes to detect U6-snRNA and miR-159 (LNA-modified and DIG-labeled, Exiqon), respectively, were also used. Hybridization was performed at 55°C for 14 hours in an automated incubator (Intavis Bioanalytical Instruments, Köln, Germany), and followed by post-hybridization washes and DIG detection using sheep anti-DIG antibody and NBT/BCP ready-to-use tablets (both from Roche Diagnostics, Indianapolis, IN, USA).

Alternatively, fluorescent in situ hybridization (FISH) was performed for miR-200c detection, as previously described (Silahtaroglu et al., 2007), with modifications. Briefly, after the hybridization and post-hybridization steps, the glands were washed in TN buffer (0.1 M Tris-HCl pH 7.5, 0.15 M NaCl) and blocked for 1 hour (1% blocking reagent, 10% sheep serum, 1% BSA). An anti-DIG-POD (Roche Diagnostics, Indianapolis, IN, USA) and anti-E-cadherin (previously described for EdU analysis) antibodies were added for incubation for 12 hours at 4°C, followed by washes with TNT buffer (TN buffer containing 0.3% Triton X-100) and detection of E-cadherin antibody as previously described. Finally, a Cy3-tyramide reagent diluted 1:100 in amplification solution (Perkin Elmer Life Sciences, Boston, MA, USA) was incubated with the glands for 5 minutes at room temperature in the dark, followed by extensive washings in TNT buffer and whole-mount laser-scanning microscopy analysis.

Western blot

MAPK and AKT activation were detected by western blot using RIPA protein lysates after recombinant reelin and Vldlr function-blocking antibody treatments. Briefly, 1-5 μg of total protein from each treatment were loaded onto NuPAGE 4-12% polyacrylamide gels (Invitrogen, Carlsbad, CA, USA) and the proteins were separated and transferred to PVDF membranes, which were blocked in 5% BSA in TBS-T and incubated with rabbit anti-mouse antibodies to detect total and phosphorylated MAPK and PI3K (Cell Signaling Technology, Boston, MA, USA). The detection was performed using an anti-rabbit IgG HRP-linked antibody (Cell Signaling Technology) and West Dura Supersignal substrate (Thermo-Pierce, Rockford, IL, USA).

Analysis of miRNA target genes by bioinformatics

The miRNAs detected in SMGs using TLDA analysis were analyzed in the miRBase microRNA database (http://www.mirbase.org) (Griffiths-Jones et al., 2008). Target prediction was performed for miR-200c using three databases: TargetScan (http://www.targetscan.org) (Friedman, R. C. et al., 2009), Microcosm (EMBL-EBI Enright group, http://www.ebi.ac.uk/

enright-srv/microcosm) and PicTar (http://www.pictar.mdc-berlin.de) (Krek et al., 2005). After generating an aggregated list of miR-200c predicted target genes, their presence was further confirmed in the SMG by Agilent whole mouse genome microarray analysis (Agilent, Santa Clara, CA, USA). Epithelia from E13 SMGs were mechanically separated into end buds and ducts and three independent pools of RNA were analyzed. Triplicate arrays were analyzed with GeneSpring Software (Agilent, Santa Clara, CA, USA), comparing the relative fold change in expression between end buds and ducts. The array data are available in the SGMAP database (Salivary Gland Molecular Anatomy Project, http://sgmap.nidcr.nih.gov/sgmap/sgexp.html).

Branching morphogenesis, morphometric analysis and statistics

Branching morphogenesis was measured by counting the number of end buds, and the morphogenic index in epithelial cultures was calculated by multiplying the number of end buds by the length of the ducts, as previously reported (Patel et al., 2007). All SMG data were obtained using at least five SMGs per group, and each experiment was repeated three times. Data were analyzed for statistical significance using Student's *t*-test to compare two different groups, and by one-way ANOVA to compare more than two experimental groups.

RESULTS

Identification of miR-200c in the SMG epithelium, a miRNA that affects branching morphogenesis

We screened the expression of miRNAs using TaqMan low density arrays in mouse E13 SMG epithelium, mesenchyme, epithelial end buds and the main duct using total RNA isolated from these tissues (Fig. 1A; supplementary material Fig. S1A-E). We detected 35 miRNAs that were more abundant in the epithelium than in the mesenchyme (Fig. 1B; supplementary material Table S2), 116 miRNAs that were more abundant in the mesenchyme than in the epithelium (supplementary material Fig. S1C and Table S2), and 113 miRNAs that were ubiquitously expressed in both tissues (supplementary material Table S2). The corresponding gene ontology analysis of the 20 most abundant miRNAs present in the epithelium and mesenchyme is included (supplementary material Tables S3, S4). The SMG mesenchyme contains both endothelial and neuronal cells, and some of the miRNAs detected in the mesenchyme have previously been reported to be endothelial cell- and neuronal cell-specific (supplementary material Fig. S1D,E). Among the epithelial miRNAs, eight were more highly expressed in the end buds, including miR-34a and miR-200c, and six were more highly expressed in the main ducts, including miR-204 and miR-135a (Fig. 1C,D; supplementary material Table S2). Other miR-200 family members, such as miR-141, miR-200a, miR-429 and miR-200b, are ubiquitously expressed throughout the epithelium (Fig. 1E; supplementary material Table S2).

We hypothesized that these miRNAs might regulate gene expression in discrete regions of the epithelium during branching morphogenesis, and focused on the two most highly expressed miRNAs in the end buds (miR-34a and miR-200c) and in the main duct (miR-135a and miR-204). We used miRNA antagomirs in a loss-of-function approach to investigate whether these miRNAs influence branching morphogenesis. Intact E12 SMGs were cultured in the presence of a control off-target (miR-control) or miR-200c, miR-34a, miR-204 and miR-135a antagomirs, and branching morphogenesis was analyzed by counting the number of epithelial end buds after 42 hours (Fig. 1F). Loss-of-function of miR-200c and miR-34a increased the number of end buds, whereas targeting miR-204 or miR-135a decreased branching morphogenesis. Both miR-204 and miR-135a are more highly expressed in ducts, which contain progenitor cells (Knox et al., 2010), and these miRNAs may positively regulate progenitor cell growth. Since knockdown of miR-200c resulted in the greatest increase in epithelial branching, we focused on identifying its role during SMG morphogenesis.

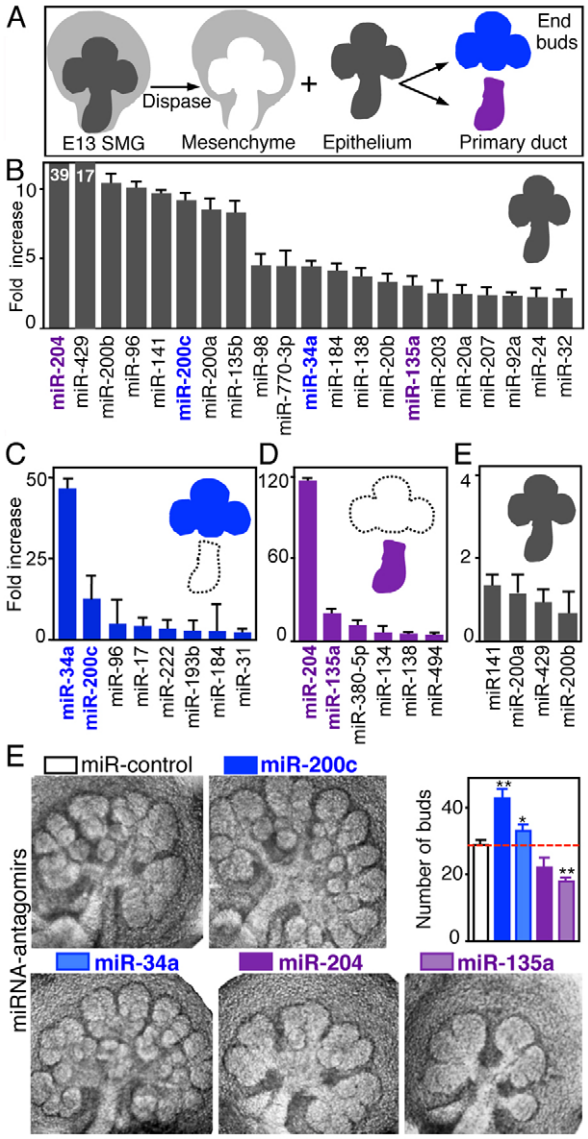

Fig. 1. Identification of miR-200c in the submandibular gland end bud epithelium, a miRNA that influences branching morphogenesis. (**A**) Mouse embryonic submandibular glands (SMGs) were separated into epithelium and mesenchyme, and end buds and primary duct, prior to miRNA expression analysis using TaqMan low density arrays. (**B-E**) Relative expression of miRNAs that show higher expression in the epithelium than in the mesenchyme (B), in the epithelial end buds than in the main duct (C), and in the main duct than in the end buds (D). The miR-200 family components are also ubiquitously expressed throughout the epithelium (E). miRNAs were selected for loss-of-function studies based on their relative expression in the end buds (miR-34a and miR-200c, blue), and in the main duct (miR-204 and miR-135a, purple). (**F**) Epithelial branching increases with miR-200c and miR-34a and decreases with miR-204 and miR-135a loss-of-function. E12 SMGs were cultured with an off-target miR-control, miR-200c, miR-34a, miR-204 and miR-135a antagomirs for 60 hours. Branching morphogenesis was quantitated by counting the number of end buds.*P<0.05, **P<0.01 (ANOVA). Error bars indicate s.e.m.

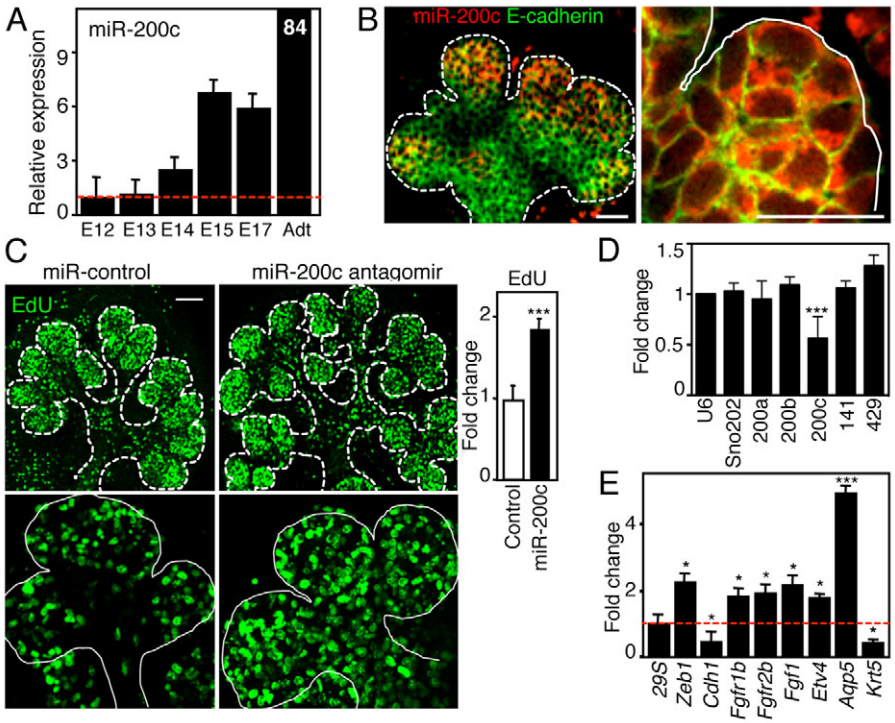

Fig. 2. The expression of miR-200c increases during SMG development, is higher in the epithelial end buds, and its loss-of-function increases proliferation during branching morphogenesis. (**A**) miR-200c expression was analyzed by qPCR throughout SMG development and normalized to expression at E12 (red line). miR-200c increases 3-fold at E14, ~6-fold at E15 and E17, and 84-fold in the adult SMG. (**B**) miR-200c was detected by fluorescent in situ hybridization (red), combined with E-cadherin immunohistochemistry (green) in E13 SMG end buds. miR-200c is localized in the cytoplasm of the epithelial tissue (right-hand image). White lines outline the epithelium. (**C**) Epithelial proliferation significantly increases with miR-200c loss-of-function. The bottom panels show higher magnification views of end buds. Proliferation was analyzed by EdU incorporation (green) and normalized to the epithelial area (bar chart). (**D**) The miR-200c antagomir specifically reduces expression of miR-200c and does not reduce expression of other miR-200 family members. SMGs were analyzed by TaqMan PCR, normalized to snRNA-U6 expression, 18 hours after antagomir treatment. (**E**) Gene expression was analyzed after antagomir treatment and normalized to *29S*. There is decreased expression (fold change) of the epithelial marker *Cdh1* (0.6) and the epithelial progenitor marker *Krt5* (0.5), and increased expression of *Fgfr1b* (2.0), *Fgfr2b* (2.0), *Fgf1* (2.4), *Etv4* (1.8) and *Aqp5* (5.0) as compared with the miR-control (red line). **P*<0.05, ***P*<0.01, ****P*<0.001 (ANOVA). Error bars indicate s.e.m. Scale bars: 20 μm in B; 50 μm in C.

The expression of miR-200c increases during SMG development, is higher in the epithelial end buds, and its loss-of-function increases proliferation during branching morphogenesis

We analyzed miR-200c expression throughout SMG development by qPCR, and normalized its expression to a housekeeping gene (snRNA-U6) and to the initial stage of gland development (E12) before branching morphogenesis began. The expression of miR-200c increased from E14 to E15, when the SMG epithelium is rapidly proliferating, and then further increased by 84-fold in the adult tissue (Fig. 2A). We confirmed the localization of miR-200c expression in E13 epithelial end buds using fluorescent in situ hybridization (FISH) and E-cadherin staining to highlight the cell-cell junctions (Fig. 2B). Our results demonstrate that miR-200c expression is highest within the epithelial end buds.

We also measured an increase in proliferation 48 hours after miR-200c loss-of-function using EdU incorporation (Fig. 2C). Since an antagomir could inhibit miRNA families with high sequence homology in their seeding or targeting sequences, we investigated whether the effect of the miR-200c antagomir was specific. We measured the expression of other miR-200 family members (Peter, 2009) using TaqMan microRNA assays 18 hours after miR-200c antagomir treatment (Fig. 2D). Whereas the expression of miR-200c was significantly reduced, the expression of other miR-200 family members did not significantly change.

Since miR-200c regulates E-cadherin (*Cdh1*), a marker of epithelial identity, by directly targeting its transcriptional repressor *Zeb1* (Gregory et al., 2008), we also analyzed these genes as positive controls to monitor the efficiency of miR-200c loss-of-function in our experiments. As expected, the direct target *Zeb1* was upregulated and *Cdh1* was downregulated after miR-200c loss-of-function (Fig. 2E). We also analyzed the expression of the FGF signaling components *Fgfr1b*, *Ffgr2b*, *Fgf1* and *Etv4*, which are involved in epithelial proliferation (Rebustini et al., 2007; Rebustini et al., 2009), and assessed the differentiation status of the epithelium by measuring the expression of the end bud marker *Aqp5* (Wei et al., 2007; Patel et al., 2008) and the progenitor cell marker *Krt5* (Knox et al., 2010). The expression of *Fgfr1b*, *Ffgr2b*, *Fgf1*, *Etv4* and *Aqp5* increased, whereas *Krt5* decreased (Fig. 2E). Our experiments using intact SMGs showed that miR-200c loss-of-function increases epithelial proliferation and the expression of FGFR signaling components and *Etv4*, which is a direct transcriptional target of Fgf10/Fgfr2b signaling in the SMG (Lombaert and Hoffman, 2010). The decrease in *Krt5* and the increase in *Aqp5* expression suggest that cell differentiation is also taking place.

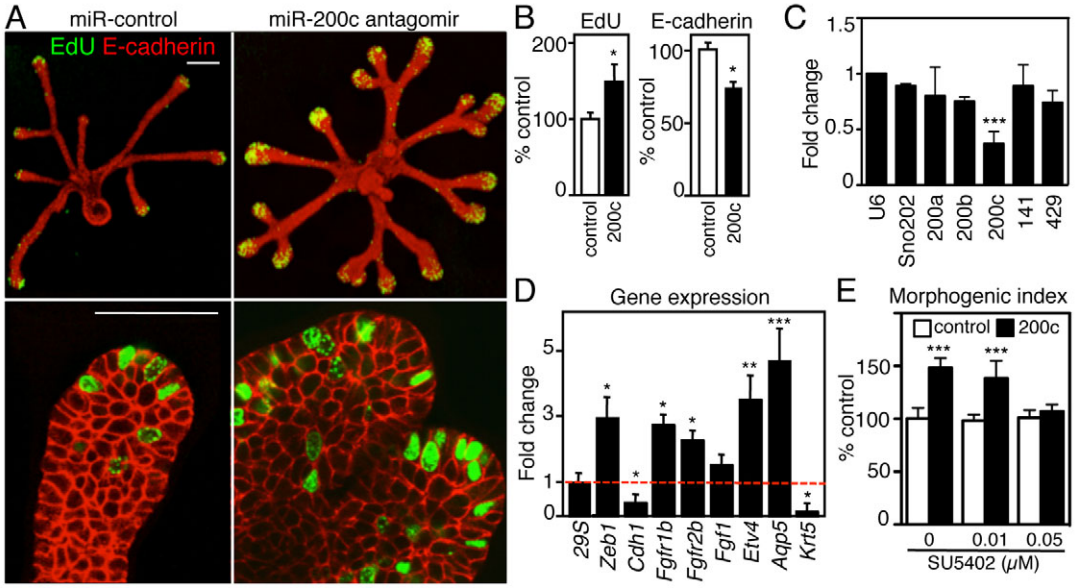

Fig. 3. Loss-of-function of miR-200c in the epithelium increases Fgf10-dependent proliferation and the expression of genes associated with Fgf10/Fgfr2b signaling. SMG epithelia were cultured with antagomirs for 42 hours. (**A**) miR-200c loss-of-function increases epithelial branching morphogenesis and proliferation as determined by EdU incorporation (top panels) and reduces E-cadherin staining (bottom panels). Scale bar: 50 μm. (**B**) Quantification of fluorescence after miR-200c loss-of-function in the epithelia, normalized to miR-control. **P*<0.05 (Student's *t*-test). (**C**) The miR-200c antagomir specifically reduces expression of miR-200c and does not reduce expression of other miR-200 family members. SMGs were analyzed by TaqMan PCR, normalized to snRNA-U6 expression, 42 hours after antagomir treatment. ****P*<0.001 (ANOVA). (**D**) miR-200c loss-of-function increases the expression (fold change) of *Fgfr1b* (3.0), *Fgfr2b* (2.7), *Fgf1* (2.0), *Etv4* (4.1), *Zeb1* (3.1), *Aqp5* (4.9), and decreases expression of *Cdh1* (0.6) and the epithelial progenitor cell marker *Krt5* (0.3). Expression was normalized to *29S* and compared with miR-control (red line). **P*<0.05, ***P*<0.01, ****P*<0.001 (ANOVA). (**E**) The increase in epithelial morphogenesis after miR-200c antagomir treatment is dependent on FGFR signaling. Morphogenic index = number of buds × length of ducts in arbitrary units, normalized to untreated control epithelia. SU5402 inhibits FGFR phosphorylation. Error bars indicate s.e.m.

To confirm that miR-200c regulates Fgf10-dependent epithelial proliferation, we analyzed miR-200c function in isolated SMG epithelium.

Loss-of-function of miR-200c increases Fgf10-dependent epithelial proliferation and the expression of genes associated with Fgf10/Fgfr2b signaling

We cultured isolated SMG epithelium in 3D laminin matrix in the presence of Fgf10 (Rebustini and Hoffman, 2009) with either control or miR-200c antagomirs. E-cadherin and cell proliferation were detected by immunostaining and EdU incorporation, respectively. After miR-200c loss-of-function, both epithelial morphogenesis and end bud proliferation increased, whereas E-cadherin decreased (Fig. 3A,B). We measured the expression of other miR-200c family members by TaqMan PCR after miR-200c antagomir treatment (Fig. 3C). The expression of miR-200c was significantly reduced, whereas the expression of other miR-200 family members did not significantly change. We used qPCR to measure gene expression associated with epithelial proliferation, FGFR signaling and differentiation (Fig. 3D), which recapitulated our findings from intact SMG cultures (Fig. 2E). The expression of *Fgfr1b*, *Ffgr2b*, *Fgf1*, *Etv4* and *Aqp5* increased, whereas *Krt5* and *Cdh1* decreased. The increase in *Etv4*, which is downstream of Fgfr2b signaling, suggests that FGFR signaling is influenced by mir-200c antagomir treatment. We also detected an increase in the amount of epithelial morphogenesis after miR-200c antagomir treatment, and the addition of SU5402, an inhibitor of FGFR signaling, reduced the miR-200c-dependent increase in morphogenesis (Fig. 3E). Taken together, our findings confirmed that loss-of-function of miR-200c in the epithelium increases Fgf10-dependent proliferation and demonstrates that FGFR signaling is required for the miR-200c-dependent increase in morphogenesis. The reduction of *Krt5* and the increase in *Aqp5* suggested that the epithelium differentiates when miR-200c function is reduced. However, none of the genes analyzed is predicted to be a direct target of miR-200c. Therefore, in order to identify the mechanism connecting miR-200c function with FGFR-dependent proliferation and *Krt5* or *Aqp5* expression, we needed to identify and confirm potential miR-200c target genes in the SMG that might control these processes.

Expression of the predicted target genes *Vldlr* and *Hs3st1* is localized in the epithelial end buds and increases after miR-200c loss-of-function

We identified potential miR-200c target genes using three prediction databases: MicroCosm, TargetScan and PicTar (supplementary material Fig. S2), and generated a list of 36 genes (supplementary material Table S5) predicted by these three programs. We analyzed the expression of these genes throughout SMG development using a public microarray database, the Salivary Gland Molecular Anatomy Project (http://sgmap.nidcr.nih.gov/sgmap/sgexp.html), and confirmed the expression of 31 of the target genes by qPCR. We also compared the relative expression of these 31 target genes in E13 SMG epithelial end buds compared with the main duct by microarray analysis (Fig. 4A). Two of the predicted targets, *Vldlr* and *Hs3st1*, were more highly expressed in the epithelial end buds than in the duct (Fig. 4A). In order to confirm that the 31 genes were

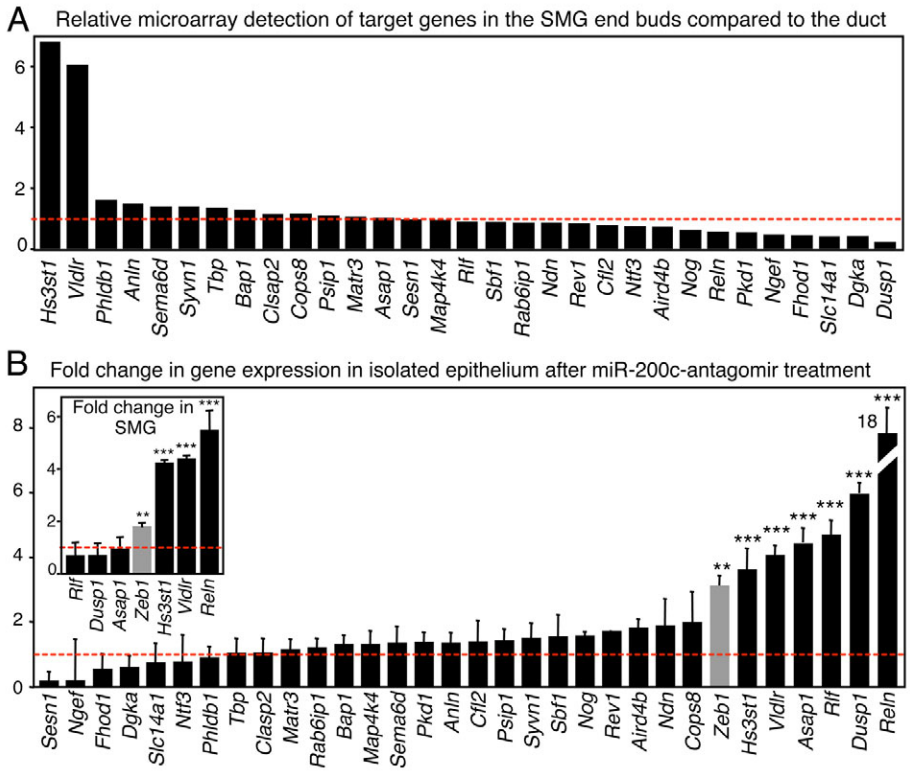

Fig. 4. Expression of the predicted miR-200c target genes *Vldlr* and *Hs3st1* is localized in the epithelial end buds and increases after miR-200c loss-of-function. Target genes for miR-200c were predicted using MicroCosm, TargetScan and PicTar databases (supplementary material Fig. S2 and Table S5), and their relative expression in E13 SMG was verified in the SGMAP database. (**A**) Microarray analysis comparing the fold change in gene expression of predicted miR-200c target genes in the epithelial end buds compared with the main duct detects *Vldlr* and *Hs3st1* expression in the end buds. The red line represents genes that are expressed equally in the epithelial end buds and in the main duct. (**B**) Gene expression (fold change) of predicted targets was measured 18 hours after antagomir treatment in isolated epithelia and intact SMGs (inset). miR-200c loss-of-function increases expression of *Hs3st1* (4.0), *Vldlr* (4.2), *Reln* (18.0), *Zeb1* (3.7), *Asap1* (4.6), *Dusp1* (7.0) and *Rlf* (4.8). The inset shows gene expression of miR-200c target genes in the intact SMG: *Reln* (5.4), *Vldlr* (4.6), *Hs3st1* (4.5) and *Zeb1* (1.9). *Zeb1* is a positive control for miR-200c loss-of-function and is shown in gray. $^{**}P<0.01$, $^{***}P<0.001$ (Student's *t*-test). Error bars indicate s.e.m.

potential targets of miR-200c in the SMG epithelium, we analyzed their expression by qPCR after miR-200c loss-of-function by antagomir treatment of isolated SMG epithelium (Fig. 4B). We found a significant increase in expression (fold change) of *Vldlr* (4.2), *Hs3st1* (4.0), *Asap1* (4.6), *Rlf* (4.8), *Dusp1* (7.0) and *Reln* (18) after 18 hours of antagomir treatment. *Zeb1* (3.7), which is a known target for miR-200c, was used as a positive control to check for miR-200c loss-of-function. Conversely, we also detected a reduction in expression of the same target genes in gain-of-function experiments using a miR-200c mimic in epithelial cultures (supplementary material Fig. S3A). In addition, we detected an increase in the expression of these target genes after 18 hours of miR-200c loss-of-function using antagomirs in the intact SMG (Fig. 4B, inset), and a decrease in expression using the corresponding miR-200c mimic (supplementary material Fig. S3B). Thus, we confirmed that miR-200c targets the expression of *Vldlr* and *Hs3st1*, which are expressed in the epithelial end buds, and identified other target genes such as *Dusp1*, *Asap1* and *Rlf*; these other target genes are involved in the regulation of MAPK signaling (Calvisi et al., 2008; Lin et al., 2008), proliferation during prostate cancer (Lin et al., 2008), and inhibition of embryonic stem cell differentiation (MacLean-Hunter et al., 1994), respectively. In addition, we confirmed that the VLDR ligand *Reln* is also a miR-200c target gene. However, the functions of Vldlr in salivary glands have not been reported; therefore, we confirmed the protein localization in the SMG.

Vldlr is localized in the SMG end buds and Vldlr function increases epithelial proliferation and Fgfr2b-dependent gene expression

Whole-mount immunostaining confirmed the presence and distribution of Vldlr in the epithelial end buds of E13 SMGs and showed punctate localization within epithelial cells and in the cell membranes along with E-cadherin (Fig. 5A). Since miR-200c loss-of-function increased both Vldlr and reelin, we hypothesized that Vldlr function regulates the expression of Fgfr2b signaling components and influences epithelial proliferation. To test our hypothesis, we used both gain- and loss-of-function of Vldlr. We directly stimulated Vldlr with recombinant reelin (Sinagra et al., 2005) and used a Vldlr function-blocking antibody (Oganesian et al., 2008) to inhibit Vldlr activity (Fig. 5B). Proliferation was measured by EdU incorporation in E12 SMGs treated with reelin and the Vldlr function-blocking antibody. Both branching morphogenesis and epithelial proliferation increased with reelin treatment and both decreased with Vldlr function-blocking antibody treatment (Fig. 5B). Analysis of gene expression by qPCR showed that *Fgfr1b*, *Fgfr2b*, *Etv4* and *Aqp5* increased with reelin treatment and decreased with Vldlr function-blocking antibodies (Fig. 5C). We found that gain- and loss-of-function of Vldlr influences proliferation and FGFR gene expression in SMGs, and investigated whether the mechanism involved miR-200c function directly in the epithelium.

The increase in epithelial proliferation and the expression of Fgfr2b signaling components with miR-200c antagomir treatment are Vldlr dependent

To directly test the effects of gain- and loss-of-function of Vldlr we used isolated SMG epithelia cultured with Fgf10. We analyzed epithelial proliferation by EdU detection after antagomir treatment, comparing miR-200c with a miR-control antagomir (Fig. 6A-F). Epithelia treated with reelin exhibited a dose-dependent increase in proliferation (Fig. 6B,C). Importantly, the Vldlr function-blocking antibody inhibited both epithelial morphogenesis and proliferation induced by the miR-200c antagomir (Fig. 6E,F), and the epithelia resembled the control treatment (Fig. 6A). We also measured the

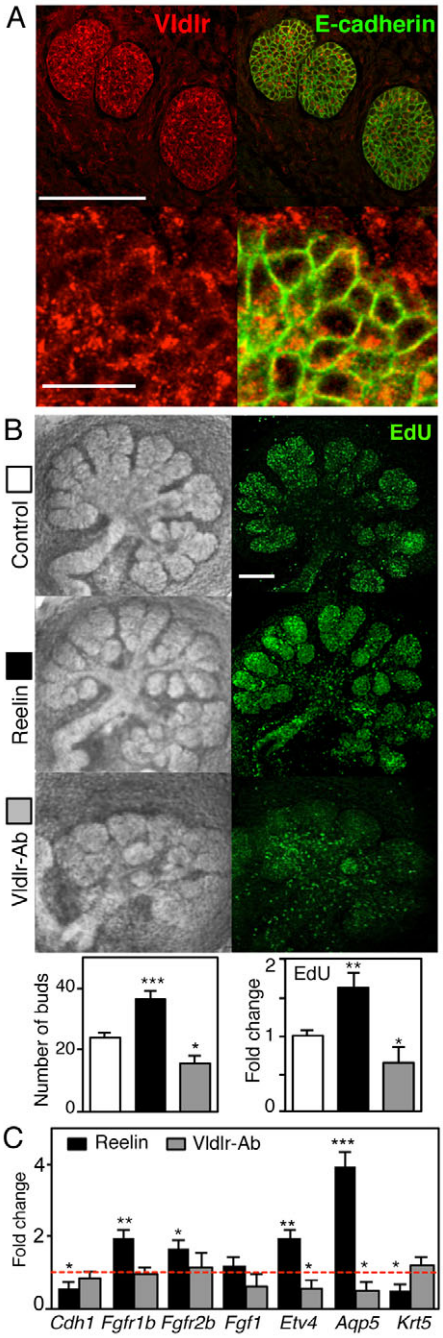

Fig. 5. Vldlr function influences epithelial proliferation and Fgfr2b-dependent gene expression in the intact SMG. (**A**) Vldlr was detected in SMG epithelial end buds. The single laser-scanning microscopy sections show that Vldlr localizes in the epithelial end bud (left panels). E-cadherin (green) and VLDR (red) are shown together in the right panels. (**B**) SMGs were cultured with reelin and a Vldlr function-blocking antibody, and proliferation was detected by EdU incorporation after 24 hours. Reelin increases, whereas a Vldlr-blocking antibody decreases, branching morphogenesis and proliferation. The bar charts beneath show quantitation of branching morphogenesis and proliferation. (**C**) Gene expression analysis after reelin and Vldlr function-blocking antibody treatments was performed by qPCR. Recombinant reelin and Vldlr function-blocking antibody showed opposite effects on the expression of *Cdh1*, *Fgfr1b*, *Fgfr2b*, *Fgf1*, *Etv4*, *Aqp5* and *Krt5*. The data were normalized to *29S* and control treatment (red line). **P*<0.05, ***P*<0.01, ****P*<0.001 (ANOVA). Scale bars: 100 μm in A top and B; 10 μm in A bottom. Error bars indicate s.e.m.

endogenous expression of miR-200c after reelin, miR-200c antagomir and anti-Vldlr antibody treatment (Fig. 6G). As expected, the antagomir treatment downregulated miR-200c expression. Surprisingly, reelin treatment reduced miR-200c expression and the Vldlr-function blocking antibodies increased miR-200c expression ~2-fold above control levels. These data suggest that Vldlr function also regulates miR-200c expression.

The morphology of the epithelia treated with recombinant reelin at 100 ng/ml resembled that of epithelia treated with the miR-200c antagomir (Fig. 6B,D), and we predicted that the downstream gene expression after reelin treatment would be similar to that following miR-200c antagomir treatment (Fig. 6H). Accordingly, reelin treatment increased the expression (fold change) of *Fgfr1b* (2.1), *Fgfr2b* (1.9), *Etv4* (2.1) and *Aqp5* (4.0), and decreased *Cdh1* (0.5) and *Krt5* (0.4) expression, as assessed by qPCR. These results suggest that exogenous reelin treatment mimics miR-200c loss-of-function, and supports our hypothesis that the downstream effect of miR-200c on Fgfr2b-mediated proliferation is mediated by Vldlr function.

In addition, MAPK signaling is downstream of Fgf10/Fgfr2b signaling during SMG epithelial proliferation (Steinberg et al., 2005; Rebustini et al., 2009); therefore, we investigated whether PI3K and MAPK were affected after gain- and loss-of-function of Vldlr. SMG epithelia were treated with recombinant reelin or Vldlr function-blocking antibodies and analyzed for MAPK and AKT phosphorylation. As expected from our previous work on FGFR signaling in the SMG epithelium (Steinberg et al., 2005), MAPK but not AKT phosphorylation was reduced by the Vldlr function-blocking antibody and stimulated by recombinant reelin at 24 hours (Fig. 6I). Taken together, these data demonstrate that the increase in both FGFR gene expression and epithelial proliferation are Vldlr dependent, and that feedback from Vldlr influences miR-200c expression. We conclude that a miR-200c-regulated Vldlr function plays a role by regulating FGFR signaling and proliferation in the intact SMG during branching morphogenesis.

DISCUSSION

We have discovered a functional role for miR-200c in controlling epithelial end bud proliferation during branching morphogenesis. In our working model (Fig. 7), miR-200c regulates genes that alter Vldlr function, which affects the expression of downstream FGFR-dependent genes and proliferation. In addition, miR-200c targets *Zeb1* and *Cdh1* expression, both involved in epithelial differentiation. In our model, we show E-cadherin separate to reelin/Vldlr signaling; however, a potential link between these two signaling systems would likely be β-catenin, which is downstream of E-cadherin and is also reported to be downstream to reelin/Vldlr signaling (He et al., 2010). We focused our studies on miR-200c based on its high expression in discrete regions of the epithelium (Fig. 1B,C, Fig. 2B), its relative abundance throughout SMG development (Fig. 2A), and on the striking induction of morphogenesis and proliferation caused by its loss-of-function (Fig. 1F). We also demonstrated that *Vldlr* and *Hs3st1* are targeted by miR-200c in the end buds (Fig. 4). Furthermore, we determined that inhibiting Vldlr function increases, and stimulating Vldlr with reelin decreases, miR-200c expression (Fig. 6). These data suggest a feedback loop between miR-200c regulation of *Vldlr* and Vldlr function regulating miR-200c expression. We propose that miR-200c provides a mechanism to negatively regulate proliferation and premature differentiation in the SMG end buds as the organ enlarges during branching morphogenesis.

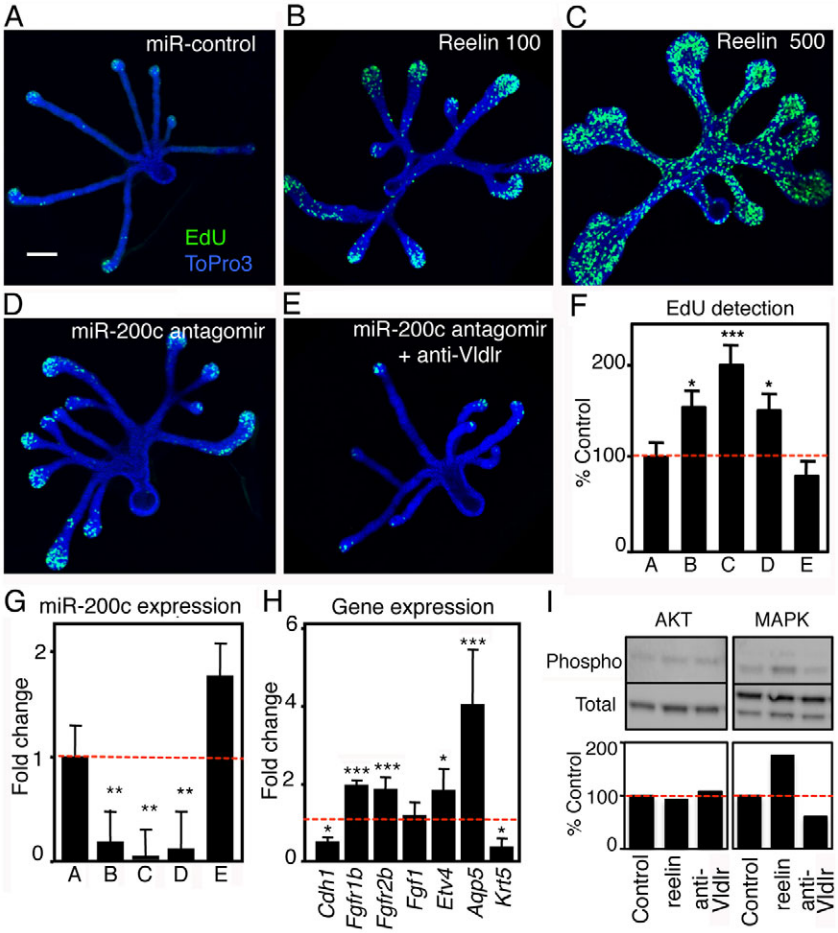

Fig. 6. Increased epithelial proliferation with miR-200c antagomir is Vldlr- and MAPK-dependent, and reelin treatment recapitulates miR-200c loss-of-function. (**A-E**) Epithelial proliferation was analyzed by EdU incorporation after (A) miR-control treatment, (B) 100 ng/ml reelin, (C) 500 ng/ml reelin, (D) miR-200c antagomir, and (E) a combination of miR-200c antagomir and anti-Vldlr function-blocking antibody. (**F**) Quantitation of proliferation normalized to nuclei staining and miR-control treatment. (**G**) qPCR analysis shows a decrease in miR-200c expression after reelin and miR-200c antagomir treatments and an increase with Vldlr function-blocking antibody treatment. (**H**) Reelin treatment (as in D) reduces gene expression (fold change) of *Cdh1* (0.5) and *Krt5* (0.4), and increases *Fgfr1b* (2.1), *Fgfr2b* (2.0), *Etv4* (2.0) and *Aqp5* (3.8). qPCR analysis was normalized to *29S* and miR-control. (**I**) The Vldlr function-blocking antibody reduces, and recombinant reelin stimulates, MAPK activation after 24 hours. The bar charts show the ratio (normalized to control treatment) of phospho-MAPK to total MAPK (right) and phospho-AKT to total AKT (left). **P*<0.05, ***P*<0.01, ****P*<0.001 (ANOVA). Scale bar: 50 μm.

Our finding that miR-200c decreases proliferation during epithelial morphogenesis corroborates previous observations on the role of miR-200c and Vldlr function during cancer formation. miR-200c is downregulated or silenced in epithelial tumors (Burk et al., 2008; Shimono et al., 2009), increased Vldlr expression is also associated with cancer metastasis (He et al., 2010), and *Reln* is abnormally overexpressed in epithelial tumors (Perrone et al., 2007). We report that miR-200c reduces *Vldlr* and *Reln* expression in the epithelial end buds and consequently reduces FGFR-dependent proliferation, thus counterbalancing the proliferative signals from FGFR signaling during development. We also demonstrate that stimulation of Vldlr decreases miR-200c expression, but whether a similar feedback occurs during epithelial tumor formation is not known. Interestingly, the promoters for both *Mir200c* and *Reln* are epigenetically regulated by methylation in cancer (Dohi et al., 2010; Vrba et al., 2010), although it remains to be investigated whether *Mir200c* is subject to epigenetic regulation during organ development.

Among the 31 predicted miR-200c target genes present in the SMG (Fig. 4A), we validated seven genes using a miR-200c loss-of-function approach (supplementary material Fig. S3) followed by qPCR analysis (Fig. 4B). This result is in accordance with the relatively low success rate for the prediction of target genes using bioinformatics databases (Doran and Strauss, 2007). In addition, the use of an aggregated list containing only target genes detected by all three prediction databases (TargetScan, PicTar and MicroCosm; supplementary material Fig. S2) proved to be highly stringent. Interestingly, *Zeb1*, *Sox2* and *Klf4*, which are targeted by miR-200c (Wellner et al., 2009) and increased in expression with antagomir treatment in SMG epithelium (supplementary material Fig. S4), were only predicted by two out of three databases (supplementary material Table S5). However, the presence of the binding sites for the miR-200c seeding region at the 3′UTR in *Zeb1*, *Vldlr*, *Hs3st1* and *Reln* mRNAs (supplementary material Fig. S5) suggests that these might be miR-200c targets. Their expression increased after miR-200c antagomir treatment and decreased with the miR-200c mimic treatments in both epithelial culture and intact SMGs (supplementary material Fig. S3). We also detected an increase in the expression of the pro-proliferative targets *Dusp1* (Calvisi et al., 2008; Lin et al., 2008), *Asap1* (Lin et al., 2008) and *Rlf* (MacLean-Hunter et al., 1994) after miR-200c loss-of-function in isolated epithelia (Fig. 4B) but not in intact SMGs (Fig. 4B, inset). Expression of these genes is more abundant in the mesenchyme and might be controlled by other mesenchymal factors, rather than by miR-200c expressed in the epithelium.

Our data suggest a role for reelin, which is highly expressed in neuronal tissues (Herz et al., 2006), in modulating neuronal-epithelial crosstalk during SMG branching morphogenesis. We previously demonstrated that the innervation of the developing SMG maintains the Krt5-positive epithelial progenitor cells during branching morphogenesis (Knox et al., 2010). Thus, reelin binding to Vldlr could influence the differentiation status of the epithelium. We found that *Krt5*, *Krt15* and *Aqp3* expression associated with basal progenitor cells decreased with miR-200c loss-of-function, whereas the epithelial differentiation marker *Aqp5* increased (Figs 4, 5; supplementary material Fig. S4), suggesting that miR-200c might be involved in epithelial progenitor cell differentiation in the end buds. In addition, others have demonstrated that miR-200c is

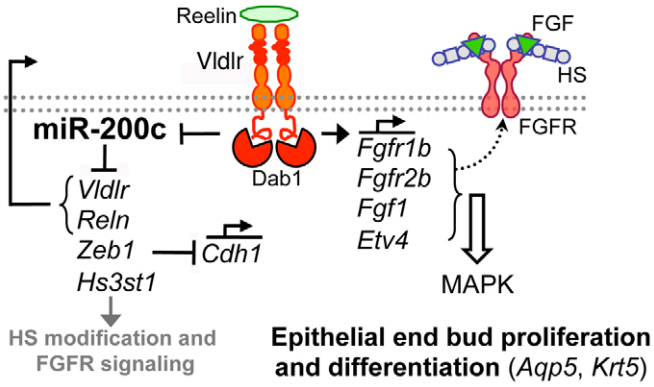

Fig. 7. miR-200c counterbalances proliferation by regulating Vldlr-dependent expression of FGFR genes during epithelial branching morphogenesis. We propose that miR-200c targets *Vldlr* function by decreasing *Vldlr* and *Reln* expression, which counterbalances FGF-dependent proliferation and differentiation in the epithelial end buds. Dab1 is the intracellular adapter protein that transduces Vldlr signaling and *Dab1*$^{-/-}$ mice have smaller SMGs than control mice (supplementary material Fig. S6). Our working model also includes the previously described miR-200c target genes *Zeb1* and *Hs3st1*, which regulate *Cdh1* and heparan sulfate (HS) modification, respectively (gray). Genes associated with epithelial cell identity (*Cdh1*), progenitor maintenance (*Krt5*) and end bud differentiation (*Aqp5*) are downstream to miR-200c.

highly expressed in primitive embryonic stem cells (Spruce et al., 2010) and targets *Sox2*, *Nanog* and *Klf4* (Wellner et al., 2009). We also demonstrated that after miR-200c loss-of-function *Sox2* and *Klf4* are upregulated (supplementary material Fig. S4). Since mammary gland ductal morphogenesis is reduced in both *Reln*$^{-/-}$ and *Dab1*$^{-/-}$ mice (Khialeeva et al., 2011), we analyzed the SMGs in *Dab1*$^{-/-}$ mice, which are 36% smaller than those of wild-type controls and also have reduced ductal morphogenesis (supplementary material Fig. S6). In the mammary gland there was an increase in Krt14-positive basal cells, demonstrating that differentiation was disrupted (Khialeeva et al., 2011). Accordingly, we detected a decrease in *Krt14* after miR-200c loss-of-function when Vldlr expression increased (supplementary material Fig. S4). However, it remains to be determined whether miR-200c influences the proliferation of specific SMG progenitor cells or whether progenitor cells in the SMGs of *Dab1*$^{-/-}$ mice are disrupted.

Here, we confirmed that epithelial *Hs3st1* expression is targeted by miR-200c (Fig. 4B). *Hs3st1*, which encodes a sulfotransferase that modifies heparan sulfate (HS), is a potential miR-200c target (Hurteau et al., 2006) that is expressed in the SMG epithelial end buds (Fig. 4A). Previous studies revealed that sulfate modifications of HS influence Fgfr2b signaling and epithelial proliferation during SMG morphogenesis (Patel et al., 2008). We speculate that the effects of miR-200c on *Hs3st1* expression also influence FGFR signaling, although further investigation is required to confirm this.

We used recombinant reelin and a Vldlr function-blocking antibody as tools to investigate Vldlr function during SMG morphogenesis. Importantly, we established that Vldlr regulates the expression of the components of the FGFR signaling pathway (Fig. 5C, Fig. 6H) via MAPK (Fig. 6I), which also affected morphogenesis (Fig. 6A-E) and downstream gene expression (Fig. 6H). Although previous studies showed that reelin binds to α3β1 integrin (Dulabon et al., 2000) and that both α3- and α6-integrins are crucial for SMG morphogenesis and signal via AKT and MAPK (Rebustini et al., 2007), we did not detect changes in AKT phosphorylation using recombinant reelin or Vldlr function-blocking antibody (Fig. 6I). Since reelin is not normally abundant in the SMG epithelium, further investigations are needed to identify other ligands that may influence Vldlr, such as apolipoproteins.

In summary, we propose that miR-200c counterbalances epithelial end bud FGFR-dependent proliferation by targeting Vldlr function, and that this regulation ensures appropriate epithelial outgrowth and differentiation during SMG branching morphogenesis. We also speculate that cancer formation and the dysregulation of the miR-200c/Vldlr regulatory pathway during normal development share common mechanisms that warrant investigation in the future.

Acknowledgements
We thank Vaishali Patel, Isabelle Lombaert, Sarah Knox and Shelagh Powers for helpful discussions and critical reading of the manuscript.

Funding
The study was supported by the Intramural Research Program of the National Institute of Dental and Craniofacial Research at the National Institutes of Health. Deposited in PMC for release after 12 months.

Competing interests statement
The authors declare no competing financial interests.

Supplementary material
Supplementary material available online at
http://dev.biologists.org/lookup/suppl/doi:10.1242/dev.070151/-/DC1

References

Adam, L., Zhong, M., Choi, W., Qi, W., Nicoloso, M., Arora, A., Calin, G., Wang, H., Siefker-Radtke, A., McConkey, D. et al. (2009). miR-200 expression regulates epithelial-to-mesenchymal transition in bladder cancer cells and reverses resistance to epidermal growth factor receptor therapy. *Clin. Cancer Res.* **15**, 5060-5072.

Ahn, H. W., Morin, R. D., Zhao, H., Harris, R. A., Coarfa, C., Chen, Z. J., Milosavljevic, A., Marra, M. A. and Rajkovic, A. (2010). MicroRNA transcriptome in the newborn mouse ovaries determined by massive parallel sequencing. *Mol. Hum. Reprod.* **16**, 463-471.

Amaral, F. C., Torres, N., Saggioro, F., Neder, L., Machado, H. R., Silva, W. A., Jr, Moreira, A. C. and Castro, M. (2009). MicroRNAs differentially expressed in ACTH-secreting pituitary tumors. *J. Clin. Endocrinol. Metab.* **94**, 320-323.

Bandres, E., Agirre, X., Bitarte, N., Ramirez, N., Zarate, R., Roman-Gomez, J., Prosper, F. and Garcia-Foncillas, J. (2009a). Epigenetic regulation of microRNA expression in colorectal cancer. *Int. J. Cancer* **125**, 2737-2743.

Bandres, E., Bitarte, N., Arias, F., Agorreta, J., Fortes, P., Agirre, X., Zarate, R., Diaz-Gonzalez, J. A., Ramirez, N., Sola, J. J. et al. (2009b). microRNA-451 regulates macrophage migration inhibitory factor production and proliferation of gastrointestinal cancer cells. *Clin. Cancer Res.* **15**, 2281-2290.

Bemis, L. T., Chen, R., Amato, C. M., Classen, E. H., Robinson, S. E., Coffey, D. G., Erickson, P. F., Shellman, Y. G. and Robinson, W. A. (2008). MicroRNA-137 targets microphthalmia-associated transcription factor in melanoma cell lines. *Cancer Res.* **68**, 1362-1368.

Bonauer, A., Carmona, G., Iwasaki, M., Mione, M., Koyanagi, M., Fischer, A., Burchfield, J., Fox, H., Doebele, C., Ohtani, K. et al. (2009). MicroRNA-92a controls angiogenesis and functional recovery of ischemic tissues in mice. *Science* **324**, 1710-1713.

Bostjancic, E., Zidar, N., Stajer, D. and Glavac, D. (2009). MicroRNAs miR-1, miR-133a, miR-133b and miR-208 are dysregulated in human myocardial infarction. *Cardiology* **115**, 163-169.

Bracken, C. P., Gregory, P. A., Kolesnikoff, N., Bert, A. G., Wang, J., Shannon, M. F. and Goodall, G. J. (2008). A double-negative feedback loop between ZEB1-SIP1 and the microRNA-200 family regulates epithelial-mesenchymal transition. *Cancer Res.* **68**, 7846-7854.

Burk, U., Schubert, J., Wellner, U., Schmalhofer, O., Vincan, E., Spaderna, S. and Brabletz, T. (2008). A reciprocal repression between ZEB1 and members of the miR-200 family promotes EMT and invasion in cancer cells. *EMBO Rep.* **9**, 582-589.

Calvisi, D. F., Pinna, F., Meloni, F., Ladu, S., Pellegrino, R., Sini, M., Daino, L., Simile, M. M., De Miglio, M. R., Virdis, P. et al. (2008). Dual-specificity phosphatase 1 ubiquitination in extracellular signal-regulated kinase-mediated control of growth in human hepatocellular carcinoma. *Cancer Res.* **68**, 4192-4200.

Cariboni, A., Rakic, S., Liapi, A., Maggi, R., Goffinet, A. and Parnavelas, J. G. (2005). Reelin provides an inhibitory signal in the migration of gonadotropin-releasing hormone neurons. *Development* **132**, 4709-4718.
Carraro, G., El-Hashash, A., Guidolin, D., Tiozzo, C., Turcatel, G., Young, B. M., De Langhe, S. P., Bellusci, S., Shi, W., Parnigotto, P. P. et al. (2009). miR-17 family of microRNAs controls FGF10-mediated embryonic lung epithelial branching morphogenesis through MAPK14 and STAT3 regulation of E-cadherin distribution. *Dev. Biol.* **333**, 238-250.
Cascio, S., D'Andrea, A., Ferla, R., Surmacz, E., Gulotta, E., Amodeo, V., Bazan, V., Gebbia, N. and Russo, A. (2010). miR-20b modulates VEGF expression by targeting HIF-1 alpha and STAT3 in MCF-7 breast cancer cells. *J. Cell. Physiol.* **224**, 242-249.
Chan, L. S., Yue, P. Y., Mak, N. K. and Wong, R. N. (2009). Role of microRNA-214 in ginsenoside-Rg1-induced angiogenesis. *Eur. J. Pharm. Sci.* **38**, 370-377.
Chan, M. C., Hilyard, A. C., Wu, C., Davis, B. N., Hill, N. S., Lal, A., Lieberman, J., Lagna, G. and Hata, A. (2009). Molecular basis for antagonism between PDGF and the TGFbeta family of signalling pathways by control of miR-24 expression. *EMBO J.* **29**, 559-573.
Crawford, M., Batte, K., Yu, L., Wu, X., Nuovo, G. J., Marsh, C. B., Otterson, G. A. and Nana-Sinkam, S. P. (2009). MicroRNA 133B targets pro-survival molecules MCL-1 and BCL2L2 in lung cancer. *Biochem. Biophys. Res. Commun.* **388**, 483-489.
D'Arcangelo, G., Homayouni, R., Keshvara, L., Rice, D. S., Sheldon, M. and Curran, T. (1999). Reelin is a ligand for lipoprotein receptors. *Neuron* **24**, 471-479.
Dohi, O., Takada, H., Wakabayashi, N., Yasui, K., Sakakura, C., Mitsufuji, S., Naito, Y., Taniwaki, M. and Yoshikawa, T. (2010). Epigenetic silencing of RELN in gastric cancer. *Int. J. Oncol.* **36**, 85-92.
Doran, J. and Strauss, W. M. (2007). Bio-informatic trends for the determination of miRNA-target interactions in mammals. *DNA Cell Biol.* **26**, 353-360.
Du, Y., Xu, Y., Ding, L., Yao, H., Yu, H., Zhou, T. and Si, J. (2009). Down-regulation of miR-141 in gastric cancer and its involvement in cell growth. *J. Gastroenterol.* **44**, 556-561.
Dulabon, L., Olson, E. C., Taglienti, M. G., Eisenhuth, S., McGrath, B., Walsh, C. A., Kreidberg, J. A. and Anton, E. S. (2000). Reelin binds alpha3beta1 integrin and inhibits neuronal migration. *Neuron* **27**, 33-44.
Flynt, A. S., Li, N., Thatcher, E. J., Solnica-Krezel, L. and Patton, J. G. (2007). Zebrafish miR-214 modulates Hedgehog signaling to specify muscle cell fate. *Nat. Genet.* **39**, 259-263.
Forrest, A. R., Kanamori-Katayama, M., Tomaru, Y., Lassmann, T., Ninomiya, N., Takahashi, Y., de Hoon, M. J., Kubosaki, A., Kaiho, A., Suzuki, M. et al. (2009). Induction of microRNAs, mir-155, mir-222, mir-424 and mir-503, promotes monocytic differentiation through combinatorial regulation. *Leukemia* **24**, 460-466.
Foshay, K. M. and Gallicano, G. I. (2009). miR-17 family miRNAs are expressed during early mammalian development and regulate stem cell differentiation. *Dev. Biol.* **326**, 431-443.
Friedman, L. M., Dror, A. A., Mor, E., Tenne, T., Toren, G., Satoh, T., Biesemeier, D. J., Shomron, N., Fekete, D. M., Hornstein, E. et al. (2009). MicroRNAs are essential for development and function of inner ear hair cells in vertebrates. *Proc. Natl. Acad. Sci. USA* **106**, 7915-7920.
Friedman, R. C., Farh, K. K., Burge, C. B. and Bartel, D. P. (2009). Most mammalian mRNAs are conserved targets of microRNAs. *Genome Res.* **19**, 92-105.
Fujita, K., Mondal, A. M., Horikawa, I., Nguyen, G. H., Kumamoto, K., Sohn, J. J., Bowman, E. D., Mathe, E. A., Schetter, A. J., Pine, S. R. et al. (2009). p53 isoforms Delta133p53 and p53beta are endogenous regulators of replicative cellular senescence. *Nat. Cell Biol.* **11**, 1135-1142.
Garzon, R., Garofalo, M., Martelli, M. P., Briesewitz, R., Wang, L., Fernandez-Cymering, C., Volinia, S., Liu, C. G., Schnittger, S., Haferlach, T. et al. (2008). Distinctive microRNA signature of acute myeloid leukemia bearing cytoplasmic mutated nucleophosmin. *Proc. Natl. Acad. Sci. USA* **105**, 3945-3950.
Gessert, S., Bugner, V., Tecza, A., Pinker, M. and Kuhl, M. (2009). FMR1/FXR1 and the miRNA pathway are required for eye and neural crest development. *Dev. Biol.* **341**, 222-235.
Greco, S., De Simone, M., Colussi, C., Zaccagnini, G., Fasanaro, P., Pescatori, M., Cardani, R., Perbellini, R., Isaia, E., Sale, P. et al. (2009). Common micro-RNA signature in skeletal muscle damage and regeneration induced by Duchenne muscular dystrophy and acute ischemia. *FASEB J.* **23**, 3335-3346.
Gregory, P. A., Bert, A. G., Paterson, E. L., Barry, S. C., Tsykin, A., Farshid, G., Vadas, M. A., Khew-Goodall, Y. and Goodall, G. J. (2008). The miR-200 family and miR-205 regulate epithelial to mesenchymal transition by targeting ZEB1 and SIP1. *Nat. Cell Biol.* **10**, 593-601.
Griffiths-Jones, S., Saini, H. K., van Dongen, S. and Enright, A. J. (2008). miRBase: tools for microRNA genomics. *Nucleic Acids Res.*, **36**, D154-D158.
Hayashi, T., Koyama, N., Azuma, Y. and Kashimata, M. (2011). Mesenchymal miR-21 regulates branching morphogenesis in murine submandibular gland in vitro. *Dev. Biol.* **352**, 299-307.
He, L., Lu, Y., Wang, P., Zhang, J., Yin, C. and Qu, S. (2010). Up-regulated expression of type II very low density lipoprotein receptor correlates with cancer metastasis and has a potential link to beta-catenin in different cancers. *BMC Cancer* **10**, 601.
Hebert, C., Norris, K., Scheper, M. A., Nikitakis, N. and Sauk, J. J. (2007). High mobility group A2 is a target for miRNA-98 in head and neck squamous cell carcinoma. *Mol. Cancer* **6**, 5.
Herz, J. and Chen, Y. (2006). Reelin, lipoprotein receptors and synaptic plasticity. *Nat. Rev. Neurosci.* **7**, 850-859.
Hoffman, M. P., Kidder, B. L., Steinberg, Z. L., Lakhani, S., Ho, S., Kleinman, H. K. and Larsen, M. (2002). Gene expression profiles of mouse submandibular gland development: FGFR1 regulates branching morphogenesis in vitro through BMP- and FGF-dependent mechanisms. *Development* **129**, 5767-5778.
Hu, G. Q., Zheng, X., Zhu, H. Q. and She, Z. S. (2009). Prediction of translation initiation site for microbial genomes with TriTISA. *Bioinformatics* **25**, 123-125.
Huang, H., Xie, C., Sun, X., Ritchie, R. P., Zhang, J. and Chen, Y. E. (2010). miR-10a contributes to retinoid acid-induced smooth muscle cell differentiation. *J. Biol. Chem.* **285**, 9383-9389.
Huang, J., Zhao, L., Xing, L. and Chen, D. (2009). MicroRNA-204 regulates Runx2 protein expression and mesenchymal progenitor cell differentiation. *Stem Cells* **28**, 357-364.
Huang, Y. W., Liu, J. C., Deatherage, D. E., Luo, J., Mutch, D. G., Goodfellow, P. J., Miller, D. S. and Huang, T. H. (2009). Epigenetic repression of microRNA-129-2 leads to overexpression of SOX4 oncogene in endometrial cancer. *Cancer Res.* **69**, 9038-9046.
Hurteau, G. J., Spivack, S. D. and Brock, G. J. (2006). Potential mRNA degradation targets of hsa-miR-200c, identified using informatics and qRT-PCR. *Cell Cycle* **5**, 1951-1956.
Hurteau, G. J., Carlson, J. A., Roos, E. and Brock, G. J. (2009). Stable expression of miR-200c alone is sufficient to regulate TCF8 (ZEB1) and restore E-cadherin expression. *Cell Cycle* **8**, 2064-2069.
Itoh, T., Nozawa, Y. and Akao, Y. (2009). MicroRNA-141 and -200a are involved in bone morphogenetic protein-2-induced mouse pre-osteoblast differentiation by targeting distal-less homeobox 5. *J. Biol. Chem.* **284**, 19272-19279.
Jevnaker, A. M. and Osmundsen, H. (2008). MicroRNA expression profiling of the developing murine molar tooth germ and the developing murine submandibular salivary gland. *Arch. Oral Biol.* **53**, 629-645.
Joglekar, M. V., Parekh, V. S. and Hardikar, A. A. (2007). New pancreas from old: microregulators of pancreas regeneration. *Trends Endocrinol. Metab.* **18**, 393-400.
Jones, S. W., Watkins, G., Le Good, N., Roberts, S., Murphy, C. L., Brockbank, S. M., Needham, M. R., Read, S. J. and Newham, P. (2009). The identification of differentially expressed microRNA in osteoarthritic tissue that modulate the production of TNF-alpha and MMP13. *Osteoarthritis Cartilage* **17**, 464-472.
Jossin, Y. and Goffinet, A. M. (2007). Reelin signals through phosphatidylinositol 3-kinase and Akt to control cortical development and through mTor to regulate dendritic growth. *Mol. Cell. Biol.* **27**, 7113-7124.
Kano, M., Seki, N., Kikkawa, N., Fujimura, L., Hoshino, I., Akutsu, Y., Chiyomaru, T., Enokida, H., Nakagawa, M. and Matsubara, H. (2011). miR-145, miR-133a and miR-133b: tumor-suppressive miRNAs target FSCN1 in esophageal squamous cell carcinoma. *Int. J. Cancer* **127**, 2804-2814.
Khialeeva, E., Lane, T. F. and Carpenter, E. M. (2011). Disruption of reelin signaling alters mammary gland morphogenesis. *Development* **138**, 767-776.
Kim, J., Inoue, K., Ishii, J., Vanti, W. B., Voronov, S. V., Murchison, E., Hannon, G. and Abeliovich, A. (2007). A MicroRNA feedback circuit in midbrain dopamine neurons. *Science* **317**, 1220-1224.
Kloosterman, W. P., Wienholds, E., de Bruijn, E., Kauppinen, S. and Plasterk, R. H. (2006). In situ detection of miRNAs in animal embryos using LNA-modified oligonucleotide probes. *Nat. Methods* **3**, 27-29.
Knox, S. M., Lombaert, I. M., Reed, X., Vitale-Cross, L., Gutkind, J. S. and Hoffman, M. P. (2010). Parasympathetic innervation maintains epithelial progenitor cells during salivary organogenesis. *Science* **329**, 1645-1647.
Kong, D., Li, Y., Wang, Z., Banerjee, S., Ahmad, A., Kim, H. R. and Sarkar, F. H. (2009). miR-200 regulates PDGF-D-mediated epithelial-mesenchymal transition, adhesion, and invasion of prostate cancer cells. *Stem Cells* **27**, 1712-1721.
Kozaki, K., Imoto, I., Mogi, S., Omura, K. and Inazawa, J. (2008). Exploration of tumor-suppressive microRNAs silenced by DNA hypermethylation in oral cancer. *Cancer Res.* **68**, 2094-2105.
Krek, A., Grun, D., Poy, M. N., Wolf, R., Rosenberg, L., Epstein, E. J., MacMenamin, P., da Piedade, I., Gunsalus, K. C., Stoffel, M. et al. (2005). Combinatorial microRNA target predictions. *Nat. Genet.* **37**, 495-500.
Lal, A., Navarro, F., Maher, C. A., Maliszewski, L. E., Yan, N., O'Day, E., Chowdhury, D., Dykxhoorn, D. M., Tsai, P., Hofmann, O. et al. (2009). miR-24 Inhibits cell proliferation by targeting E2F2, MYC, and other cell-cycle genes via binding to "seedless" 3'UTR microRNA recognition elements. *Mol. Cell* **35**, 610-625.
Lee, D. Y., Shatseva, T., Jeyapalan, Z., Du, W. W., Deng, Z. and Yang, B. B. (2009). A 3'-untranslated region (3'UTR) induces organ adhesion by regulating miR-199a* functions. *PLoS ONE* **4**, e4527.

Li, Y., VandenBoom, T. G., 2nd, Kong, D., Wang, Z., Ali, S., Philip, P. A. and Sarkar, F. H. (2009). Up-regulation of miR-200 and let-7 by natural agents leads to the reversal of epithelial-to-mesenchymal transition in gemcitabine-resistant pancreatic cancer cells. *Cancer Res.* **69**, 6704-6712.
Lian, J., Zhang, X., Tian, H., Liang, N., Wang, Y., Liang, C., Li, X. and Sun, F. (2009). Altered microRNA expression in patients with non-obstructive azoospermia. *Reprod. Biol. Endocrinol.* **7**, 13.
Lin, C. H., Jackson, A. L., Guo, J., Linsley, P. S. and Eisenman, R. N. (2009). Myc-regulated microRNAs attenuate embryonic stem cell differentiation. *EMBO J.* **28**, 3157-3170.
Lin, D., Watahiki, A., Bayani, J., Zhang, F., Liu, L., Ling, V., Sadar, M. D., English, J., Fazli, L., So, A. et al. (2008). ASAP1, a gene at 8q24, is associated with prostate cancer metastasis. *Cancer Res.* **68**, 4352-4359.
Lin, E. A., Kong, L., Bai, X. H., Luan, Y. and Liu, C. J. (2009). miR-199a, a bone morphogenic protein 2-responsive MicroRNA, regulates chondrogenesis via direct targeting to Smad1. *J. Biol. Chem.* **284**, 11326-11335.
Lombaert, I. M. and Hoffman, M. P. (2010). Epithelial stem/progenitor cells in the embryonic mouse submandibular gland. *Front. Oral Biol.* **14**, 90-106.
MacLean-Hunter, S., Makela, T. P., Grzeschiczek, A., Alitalo, K. and Moroy, T. (1994). Expression of a rlf/L-myc minigene inhibits differentiation of embryonic stem cells and embroid body formation. *Oncogene* **9**, 3509-3517.
Marasa, B. S., Srikantan, S., Masuda, K., Abdelmohsen, K., Kuwano, Y., Yang, X., Martindale, J. L., Rinker-Schaeffer, C. W. and Gorospe, M. (2009). Increased MKK4 abundance with replicative senescence is linked to the joint reduction of multiple microRNAs. *Sci. Signal.* **2**, ra69.
Marson, A., Levine, S. S., Cole, M. F., Frampton, G. M., Brambrink, T., Johnstone, S., Guenther, M. G., Johnston, W. K., Wernig, M., Newman, J. et al. (2008). Connecting microRNA genes to the core transcriptional regulatory circuitry of embryonic stem cells. *Cell* **134**, 521-533.
Masaki, S., Ohtsuka, R., Abe, Y., Muta, K. and Umemura, T. (2007). Expression patterns of microRNAs 155 and 451 during normal human erythropoiesis. *Biochem. Biophys. Res. Commun.* **364**, 509-514.
Morton, S. U., Scherz, P. J., Cordes, K. R., Ivey, K. N., Stainier, D. Y. and Srivastava, D. (2008). microRNA-138 modulates cardiac patterning during embryonic development. *Proc. Natl. Acad. Sci. USA* **105**, 17830-17835.
Nagel, R., le Sage, C., Diosdado, B., van der Waal, M., Oude Vrielink, J. A., Bolijn, A., Meijer, G. A. and Agami, R. (2008). Regulation of the adenomatous polyposis coli gene by the miR-135 family in colorectal cancer. *Cancer Res.* **68**, 5795-5802.
Nakada, C., Matsuura, K., Tsukamoto, Y., Tanigawa, M., Yoshimoto, T., Narimatsu, T., Nguyen, L. T., Hijiya, N., Uchida, T., Sato, F. et al. (2008). Genome-wide microRNA expression profiling in renal cell carcinoma: significant down-regulation of miR-141 and miR-200c. *J. Pathol.* **216**, 418-427.
O'Donnell, K. A., Wentzel, E. A., Zeller, K. I., Dang, C. V. and Mendell, J. T. (2005). c-Myc-regulated microRNAs modulate E2F1 expression. *Nature* **435**, 839-843.
Oganesian, A., Armstrong, L. C., Migliorini, M. M., Strickland, D. K. and Bornstein, P. (2008). Thrombospondins use the VLDL receptor and a nonapoptotic pathway to inhibit cell division in microvascular endothelial cells. *Mol. Biol. Cell* **19**, 563-571.
Orom, U. A., Nielsen, F. C. and Lund, A. H. (2008). MicroRNA-10a binds the 5'UTR of ribosomal protein mRNAs and enhances their translation. *Mol. Cell* **30**, 460-471.
Park, N. J., Zhou, H., Elashoff, D., Henson, B. S., Kastratovic, D. A., Abemayor, E. and Wong, D. T. (2009). Salivary microRNA: discovery, characterization, and clinical utility for oral cancer detection. *Clin. Cancer Res.* **15**, 5473-5477.
Park, S. M., Gaur, A. B., Lengyel, E. and Peter, M. E. (2008). The miR-200 family determines the epithelial phenotype of cancer cells by targeting the E-cadherin repressors ZEB1 and ZEB2. *Genes Dev.* **22**, 894-907.
Patel, V. N., Rebustini, I. T. and Hoffman, M. P. (2006). Salivary gland branching morphogenesis. *Differentiation* **74**, 349-364.
Patel, V. N., Knox, S. M., Likar, K. M., Lathrop, C. A., Hossain, R., Eftekhari, S., Whitelock, J. M., Elkin, M., Vlodavsky, I. and Hoffman, M. P. (2007). Heparanase cleavage of perlecan heparan sulfate modulates FGF10 activity during ex vivo submandibular gland branching morphogenesis. *Development* **134**, 4177-4186.
Patel, V. N., Likar, K. M., Zisman-Rozen, S., Cowherd, S. N., Lassiter, K. S., Sher, I., Yates, E. A., Turnbull, J. E., Ron, D. and Hoffman, M. P. (2008). Specific heparan sulfate structures modulate FGF10-mediated submandibular gland epithelial morphogenesis and differentiation. *J. Biol. Chem.* **283**, 9308-9317.
Patnaik, S. K., Kannisto, E., Knudsen, S. and Yendamuri, S. (2009). Evaluation of microRNA expression profiles that may predict recurrence of localized stage I non-small cell lung cancer after surgical resection. *Cancer Res.* **70**, 36-45.
Perrone, G., Vincenzi, B., Zagami, M., Santini, D., Panteri, R., Flammia, G., Verzi, A., Lepanto, D., Morini, S., Russo, A. et al. (2007). Reelin expression in human prostate cancer: a marker of tumor aggressiveness based on correlation with grade. *Mod. Pathol.* **20**, 344-351.
Peter, M. E. (2009). Let-7 and miR-200 microRNAs: guardians against pluripotency and cancer progression. *Cell Cycle* **8**, 843-852.
Pogribny, I. P., Filkowski, J. N., Tryndyak, V. P., Golubov, A., Shpyleva, S. I. and Kovalchuk, O. (2010). Alterations of microRNAs and their targets are associated with acquired resistance of MCF-7 breast cancer cells to cisplatin. *Int. J. Cancer* **127**, 1785-1794.
Qin, W., Shi, Y., Zhao, B., Yao, C., Jin, L., Ma, J. and Jin, Y. (2010). miR-24 regulates apoptosis by targeting the open reading frame (ORF) region of FAF1 in cancer cells. *PLoS ONE* **5**, e9429.
Rane, S., He, M., Sayed, D., Yan, L., Vatner, D. and Abdellatif, M. (2010). An antagonism between the AKT and beta-adrenergic signaling pathways mediated through their reciprocal effects on miR-199a-5p. *Cell Signal.* **22**, 1054-1062.
Rebustini, I. T. and Hoffman, M. P. (2009). ECM and FGF-dependent assay of embryonic SMG epithelial morphogenesis: investigating growth factor/matrix regulation of gene expression during submandibular gland development. *Methods Mol. Biol.* **522**, 319-330.
Rebustini, I. T., Patel, V. N., Stewart, J. S., Layvey, A., Georges-Labouesse, E., Miner, J. H. and Hoffman, M. P. (2007). Laminin alpha5 is necessary for submandibular gland epithelial morphogenesis and influences FGFR expression through beta1 integrin signaling. *Dev. Biol.* **308**, 15-29.
Rebustini, I. T., Myers, C., Lassiter, K. S., Surmak, A., Szabova, L., Holmbeck, K., Pedchenko, V., Hudson, B. G. and Hoffman, M. P. (2009). MT2-MMP-dependent release of collagen IV NC1 domains regulates submandibular gland branching morphogenesis. *Dev. Cell* **17**, 482-493.
Sanderson, L. M., Boekschoten, M. V., Desvergne, B., Muller, M. and Kersten, S. (2010). Transcriptional profiling reveals divergent roles of PPARalpha and PPARbeta/delta in regulation of gene expression in mouse liver. *Physiol. Genomics* **41**, 42-52.
Schoolmeesters, A., Eklund, T., Leake, D., Vermeulen, A., Smith, Q., Force Aldred, S. and Fedorov, Y. (2009). Functional profiling reveals critical role for miRNA in differentiation of human mesenchymal stem cells. *PLoS ONE* **4**, e5605.
Shimono, Y., Zabala, M., Cho, R. W., Lobo, N., Dalerba, P., Qian, D., Diehn, M., Liu, H., Panula, S. P., Chiao, E. et al. (2009). Downregulation of miRNA-200c links breast cancer stem cells with normal stem cells. *Cell* **138**, 592-603.
Siegel, G., Obernosterer, G., Fiore, R., Oehmen, M., Bicker, S., Christensen, M., Khudayberdiev, S., Leuschner, P. F., Busch, C. J., Kane, C. et al. (2009). A functional screen implicates microRNA-138-dependent regulation of the depalmitoylation enzyme APT1 in dendritic spine morphogenesis. *Nat. Cell Biol.* **11**, 705-716.
Silahtaroglu, A. N., Nolting, D., Dyrskjot, L., Berezikov, E., Moller, M., Tommerup, N. and Kauppinen, S. (2007). Detection of microRNAs in frozen tissue sections by fluorescence in situ hybridization using locked nucleic acid probes and tyramide signal amplification. *Nat. Protoc.* **2**, 2520-2528.
Sinagra, M., Verrier, D., Frankova, D., Korwek, K. M., Blahos, J., Weeber, E. J., Manzoni, O. J. and Chavis, P. (2005). Reelin, very-low-density lipoprotein receptor, and apolipoprotein E receptor 2 control somatic NMDA receptor composition during hippocampal maturation in vitro. *J. Neurosci.* **25**, 6127-6136.
Smits, G., Mungall, A. J., Griffiths-Jones, S., Smith, P., Beury, D., Matthews, L., Rogers, J., Pask, A. J., Shaw, G., VandeBerg, J. L. et al. (2008). Conservation of the H19 noncoding RNA and H19-IGF2 imprinting mechanism in therians. *Nat. Genet.* **40**, 971-976.
Spruce, T., Pernaute, B., Di-Gregorio, A., Cobb, B. S., Merkenschlager, M., Manzanares, M. and Rodriguez, T. A. (2010). An early developmental role for miRNAs in the maintenance of extraembryonic stem cells in the mouse embryo. *Dev. Cell* **19**, 207-219.
Steinberg, Z., Myers, C., Heim, V. M., Lathrop, C. A., Rebustini, I. T., Stewart, J. S., Larsen, M. and Hoffman, M. P. (2005). FGFR2b signaling regulates ex vivo submandibular gland epithelial cell proliferation and branching morphogenesis. *Development* **132**, 1223-1234.
Sun, F., Fu, H., Liu, Q., Tie, Y., Zhu, J., Xing, R., Sun, Z. and Zheng, X. (2008). Downregulation of CCND1 and CDK6 by miR-34a induces cell cycle arrest. *FEBS Lett.* **582**, 1564-1568.
Takahashi, Y., Forrest, A. R., Maeno, E., Hashimoto, T., Daub, C. O. and Yasuda, J. (2009). MiR-107 and MiR-185 can induce cell cycle arrest in human non small cell lung cancer cell lines. *PLoS ONE* **4**, e6677.
Thatcher, E. J., Paydar, I., Anderson, K. K. and Patton, J. G. (2008). Regulation of zebrafish fin regeneration by microRNAs. *Proc. Natl. Acad. Sci. USA* **105**, 18384-18389.
Tiscornia, G. and Izpisua Belmonte, J. C. (2010). MicroRNAs in embryonic stem cell function and fate. *Genes Dev.* **24**, 2732-2741.
Trommsdorff, M., Gotthardt, M., Hiesberger, T., Shelton, J., Stockinger, W., Nimpf, J., Hammer, R. E., Richardson, J. A. and Herz, J. (1999). Reeler/Disabled-like disruption of neuronal migration in knockout mice lacking the VLDL receptor and ApoE receptor 2. *Cell* **97**, 689-701.
Tzur, G., Levy, A., Meiri, E., Barad, O., Spector, Y., Bentwich, Z., Mizrahi, L., Katzenellenbogen, M., Ben-Shushan, E., Reubinoff, B. E. et al. (2008). MicroRNA expression patterns and function in endodermal differentiation of human embryonic stem cells. *PLoS ONE* **3**, e3726.

Volinia, S., Calin, G. A., Liu, C. G., Ambs, S., Cimmino, A., Petrocca, F., Visone, R., Iorio, M., Roldo, C., Ferracin, M. et al. (2006). A microRNA expression signature of human solid tumors defines cancer gene targets. *Proc. Natl. Acad. Sci. USA* **103**, 2257-2261.

Vrba, L., Jensen, T. J., Garbe, J. C., Heimark, R. L., Cress, A. E., Dickinson, S., Stampfer, M. R. and Futscher, B. W. (2010). Role for DNA methylation in the regulation of miR-200c and miR-141 expression in normal and cancer cells. *PLoS ONE* **5**, e8697.

Walker, J. L., Menko, A. S., Khalil, S., Rebustini, I., Hoffman, M. P., Kreidberg, J. A. and Kukuruzinska, M. A. (2008). Diverse roles of E-cadherin in the morphogenesis of the submandibular gland: insights into the formation of acinar and ductal structures. *Dev. Dyn.* **237**, 3128-3141.

Wang, F. E., Zhang, C., Maminishkis, A., Dong, L., Zhi, C., Li, R., Zhao, J., Majerciak, V., Gaur, A. B., Chen, S. et al. (2010). MicroRNA-204/211 alters epithelial physiology. *FASEB J.* **24**, 1552-1571.

Wang, Q., Huang, Z., Xue, H., Jin, C., Ju, X. L., Han, J. D. and Chen, Y. G. (2008). MicroRNA miR-24 inhibits erythropoiesis by targeting activin type I receptor ALK4. *Blood* **111**, 588-595.

Wang, S., Aurora, A. B., Johnson, B. A., Qi, X., McAnally, J., Hill, J. A., Richardson, J. A., Bassel-Duby, R. and Olson, E. N. (2008). The endothelial-specific microRNA miR-126 governs vascular integrity and angiogenesis. *Dev. Cell* **15**, 261-271.

Wang, Y., Weng, T., Gou, D., Chen, Z., Chintagari, N. R. and Liu, L. (2007). Identification of rat lung-specific microRNAs by micoRNA microarray: valuable discoveries for the facilitation of lung research. *BMC Genomics* **8**, 29.

Watanabe, T., Sato, T., Amano, T., Kawamura, Y., Kawamura, N., Kawaguchi, H., Yamashita, N., Kurihara, H. and Nakaoka, T. (2008). Dnm3os, a non-coding RNA, is required for normal growth and skeletal development in mice. *Dev. Dyn.* **237**, 3738-3748.

Webb, D. J., Nguyen, D. H., Sankovic, M. and Gonias, S. L. (1999). The very low density lipoprotein receptor regulates urokinase receptor catabolism and breast cancer cell motility in vitro. *J. Biol. Chem.* **274**, 7412-7420.

Wei, C., Larsen, M., Hoffman, M. P. and Yamada, K. M. (2007). Self-organization and branching morphogenesis of primary salivary epithelial cells. *Tissue Eng.* **13**, 721-735.

Wei, J. S., Song, Y. K., Durinck, S., Chen, Q. R., Cheuk, A. T., Tsang, P., Zhang, Q., Thiele, C. J., Slack, A., Shohet, J. et al. (2008). The MYCN oncogene is a direct target of miR-34a. *Oncogene* **27**, 5204-5213.

Wellner, U., Schubert, J., Burk, U. C., Schmalhofer, O., Zhu, F., Sonntag, A., Waldvogel, B., Vannier, C., Darling, D., zur Hausen, A. et al. (2009). The EMT-activator ZEB1 promotes tumorigenicity by repressing stemness-inhibiting microRNAs. *Nat. Cell Biol.* **11**, 1487-1495.

Wheeler, G., Ntounia-Fousara, S., Granda, B., Rathjen, T. and Dalmay, T. (2006). Identification of new central nervous system specific mouse microRNAs. *FEBS Lett.* **580**, 2195-2200.

Yamamoto, S., Fukumoto, E., Yoshizaki, K., Iwamoto, T., Yamada, A., Tanaka, K., Suzuki, H., Aizawa, S., Arakaki, M., Yuasa, K. et al. (2008). Platelet-derived growth factor receptor regulates salivary gland morphogenesis via fibroblast growth factor expression. *J. Biol. Chem.* **283**, 23139-23149.

Yamamoto, Y., Kosaka, N., Tanaka, M., Koizumi, F., Kanai, Y., Mizutani, T., Murakami, Y., Kuroda, M., Miyajima, A., Kato, T. et al. (2009). MicroRNA-500 as a potential diagnostic marker for hepatocellular carcinoma. *Biomarkers* **14**, 529-538.

Yi, R., O'Carroll, D., Pasolli, H. A., Zhang, Z., Dietrich, F. S., Tarakhovsky, A. and Fuchs, E. (2006). Morphogenesis in skin is governed by discrete sets of differentially expressed microRNAs. *Nat. Genet.* **38**, 356-362.

Yi, R., Poy, M. N., Stoffel, M. and Fuchs, E. (2008). A skin microRNA promotes differentiation by repressing 'stemness'. *Nature* **452**, 225-229.

Yin, V. P., Thomson, J. M., Thummel, R., Hyde, D. R., Hammond, S. M. and Poss, K. D. (2008). Fgf-dependent depletion of microRNA-133 promotes appendage regeneration in zebrafish. *Genes. Dev.* **22**, 728-733.

Yoo, A. S., Staahl, B. T., Chen, L. and Crabtree, G. R. (2009). MicroRNA-mediated switching of chromatin-remodelling complexes in neural development. *Nature* **460**, 642-646.

Yu, J., Ryan, D. G., Getsios, S., Oliveira-Fernandes, M., Fatima, A. and Lavker, R. M. (2008). MicroRNA-184 antagonizes microRNA-205 to maintain SHIP2 levels in epithelia. *Proc. Natl. Acad. Sci. USA* **105**, 19300-19305.